

VORTEX DEPTH ANALYSIS IN AN UNBAFFLED STIRRED TANK
WITH CONCAVE BLADE IMPELLER*Thiyam Devi¹, Bimlesh Kumar², **

https:

Abstract. The present study was carried out by experimenting in a stirred tank of unbaffled system employed with concave blade impeller. In this study the influence of impeller diameter (d), tank diameter (D) and impeller clearance depth (C) on vortex depth is investigated at various impeller rotational speeds. The higher vortex depth is observed when the impeller is closer to the tank bottom. Relative vortex depth increases with the increase in the impeller diameter in all cases of impeller clearance depth at constant D . Smaller tank diameter gives higher relative vortex depth, when d is constant at different impeller clearance depths. Critical speed is found decreasing with the increase in C/D and d/D ratio. Finally, a scale up criteria for relative vortex depth has been developed, which is valid for geometrically similar conditions.

Keywords: concave blade, computational fluid dynamics, stirred tank, vortex depth.

1. Introduction

To avoid formation of a pronounced central vortex at high angular speeds by breaking undesired tangential velocity components, most industrial stirred reactors are equipped with baffles. Presence of baffles increases axial and radial velocities so guaranteeing a better circulation and faster mixing than in their absence [1]. Although baffled tanks are widely used in industrial applications, there are cases in which the use of baffled tanks may be undesirable. Removing the baffles will change the flow characteristics and therefore the mixing rate, thus altering the effectiveness of the tank design for the reaction and phase contacting processes [2, 3]. Formation of the central vortex on the liquid free surface in an unbaffled stirred tank is obvious when the vessel is operated without a top cover. Vortex is formed because of the highly swirling liquid

motion which is produced by the continuous movement of the impeller. Study of the formation of vortex in an unbaffled stirred tank is very important to understand the air-entrainment at particular power consumption. So, study of vortex formation caused by an unbaffled condition of the system is closely associated with power consumption in the system as it is widely known that the unbaffled system consumes less power [4, 5] than the baffled system. Therefore, study on vortex formation in agitated vessels to save energy in terms of power consumption is required [6]. Unbaffled systems are, in fact, employed for specific applications [4, 7], where the presence of baffles results in drawbacks [8, 9]. Baffled tanks cause dead zones, actually worsening the mixing performance of an aeration system [1]. For the food and pharmaceutical industries it is a matter of primary importance to keep the reactor, as clean as possible; in crystallization processes [10] and biological applications [11] shear and impact are to be minimized; in precipitation processes baffles may suffer from incrustation problems [12]. Scientific literature shows an increasing interest in experimental investigations towards unbaffled stirred vessels [13-25] showing better potential for some industrial use of such type of stirred reactors. Brucato *et al.* [22] found minimum power requirements for complete suspension in top-covered unbaffled vessels which are less than from corresponding baffled tanks. Literature also suggests that at the same values of mechanical power dissipation the mass transfer coefficient is higher in unbaffled vessels than that in baffled tanks [26-27].

Vortex depth can be analyzed theoretically as well as experimentally. Dimensional analysis indicates that relative vortex depth is a function of impeller speed and impeller diameter; however, it may also depends on other geometrical dimensions differing from impeller diameter. Therefore, it is required to incorporate impeller clearance depth in the analysis of vortex depth. In this study, the influence of geometrical dimensions, such as impeller diameter, tank diameter, impeller speed and impeller clearance depth on relative vortex depth with concave blade type impeller is experimentally analyzed and a scale up criterion is developed for geometrically similar systems.

¹ Department of Civil Engineering, NIT Manipur, Manipur 795004, India

² Department of Civil Engineering, IIT Guwahati, Guwahati 781039, India

* bimk@iitg.ernet.in

© Devi T., Kumar B., 2017

2. Experimental

2.1. Materials and Methods

The process dynamics based on vortex depth and power consumption has been studied on unbaffled single impeller without sparging system of concave type impeller. The influence of impeller diameter (ratio of d/D is taken as 0.2, 0.3 and 0.4), tank diameter ($D = 150$ and 200 mm) and impeller clearance depth (ratio of C/D is taken from 0.3 to 0.9 with 0.1 interval) is studied based on the process dynamic characteristics at various impeller rotational speeds. Table 1 show the geometrical dimensions used in this study. Experimental determination of vortex depth is done by processing the photographs of the vortex formation (for example the edge detection method and measure tools in MATLAB®). Fig. 1 shows the schematic diagram of an unbaffled stirred tank where the central vortex formation has taken place when the impeller is rotated with a particular speed. Experimental photographs were taken during experiments at every speed and the same photograph was used to determine the vortex depth.

2.2. Theoretical Background

Knowledge of velocity and pressure profiles in an unbaffled stirred tank with agitation can be derived from a theoretical expression of vortex depth. These profiles can be obtained by simultaneously solving the equations of motion and continuity with the corresponding boundary conditions. The continuity equation for an incompressible fluid is written as:

$$\nabla \cdot \mathbf{v} = 0 \tag{1}$$

And the equation of motion (Navier-Stokes equation) is given as:

$$\rho \frac{d\mathbf{v}}{dt} = -\nabla p + \mu \nabla^2 \mathbf{v} + \rho \mathbf{g} \tag{2}$$

The boundary conditions are as follows: (1) tangential impeller velocity is equal to liquid velocity at the liquid/impeller interface; (2) liquid velocity at the vessel wall is zero; (3) the resulting force influencing the gas-liquid interphase tends to get to the surface perpendicularly. The last condition implies as [29]:

$$\mathbf{n} \cdot \mathbf{u} = -np_0 \tag{3}$$

Table 1

Tank configuration

Dimensions	Symbol	Dimensions used in the study	Values
Height of water	H	H/D	1
Tank diameter	D		
Impeller diameter	d	d/D	0.2; 0.3; 0.4
Length of blade	l	l/d	0.25
Width of blade	b	b/d	0.2
Impeller clearance depth	C	C/D	0.3–0.9
Number of blades	n	n	6
Thickness of blade	t	t	1 mm

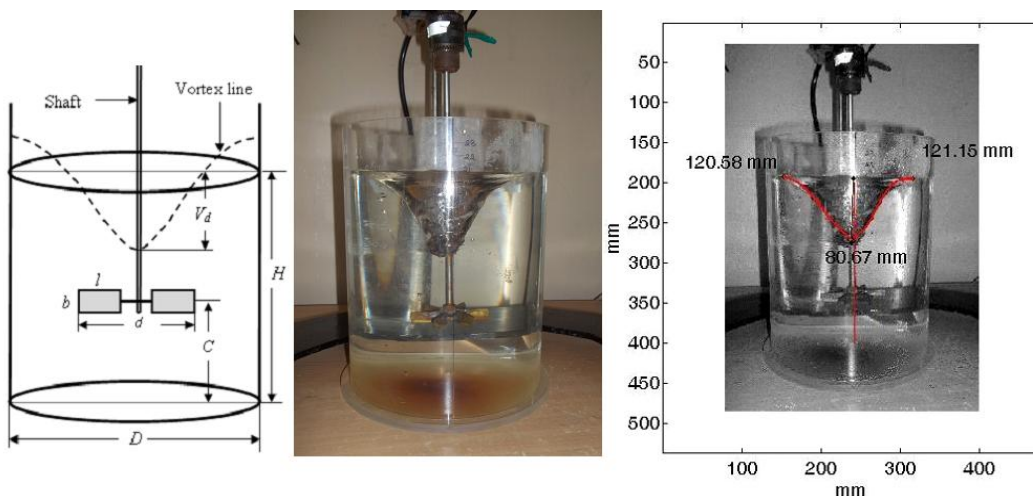


Fig. 1. Schematic diagram (left) and experimental view (centre) of the formation of vortex in an unbaffled stirred tank and vortex detected by edge detection method (right)

The analytical solution of Eqs. (1), (2) and (3) is not possible due to the geometrical complexity of impellers. Therefore, the method of dimensional analysis is used and the following dimensionless variables were introduced as:

$$\begin{aligned} \mathbf{r}^* &= \mathbf{r} / Nd, t^* = Nt, \nabla^* = d \nabla, \\ \mathbf{u}^* &= \mathbf{u} / r_w N^2 d^2, \\ g^* &= g / g, s^* = s / r_w N^2 d^2, \\ p^* &= p / r_w N^2 d^2 \end{aligned} \quad (4a-f)$$

Substituting dimensionless variables of Eq. (4a-f) into Eq. (2) and into the third boundary condition we obtain:

$$\frac{d\mathbf{v}^*}{dt^*} = -\nabla^* p^* + \frac{1}{Re} \nabla^{*2} \mathbf{v}^* + \frac{1}{Fr} \mathbf{g}^* \quad (5)$$

$$\mathbf{r} \cdot \mathbf{u}^* = -np_0^* \quad (6)$$

Using the dimensionless analysis the Eq. (5) can be written for a steady state operation as:

$$\mathbf{r}^* \cdot \mathbf{v}^* = v^*(x^*, Re, Fr) \quad \text{and} \quad p^* = p^*(x^*, Re, Fr) \quad (7a, b)$$

Combining Eqs. (6) and (7a, b) the dimensionless equation describing the vortex geometry is obtained:

$$x_L^* = x_L^*(Re, Fr) = x_L^*(Ga, Fr) \quad (8)$$

where $Ga = Re^2 / Fr$ (Galileo number). The vortex depth can be determined from Eq. (8) as the vertical parameter characterizing depth of the gas/liquid interface in the vortex centre as:

$$\frac{V_d}{d} = f(Re, Fr) = f(Ga, Fr) \quad (9)$$

Eq. (9) indicates that the relative vortex depth (V_d/d) is the function of impeller speed and impeller diameter, however, the vortex depth may also be affected by other geometrical dimensions different from impeller diameter. As the objective of this study is to analyze the dependence of impeller clearance depth on various process dynamics characteristics, it is also required to incorporate impeller clearance depth C in the analysis of vortex depth. So, by keeping other geometrical parameters as a constant one and only varying tank diameter and impeller clearance, the following dimensionless relation of vortex depth is written as:

$$\frac{V_d}{d} = f\left(\frac{D}{d}, \frac{C}{D}, Ga, Fr\right) \quad (10)$$

Markopoulos and Kontogeorgaki [6] also showed that relative vortex depth is the function of impeller diameter (d), tank diameter (D), impeller speed (N),

viscosity of fluid (ν), gravitational force (g) and impeller clearance depth (C). So, in the following sections, the influence of d , D , C and N on relative vortex depth will be discussed.

3. Results and Discussions

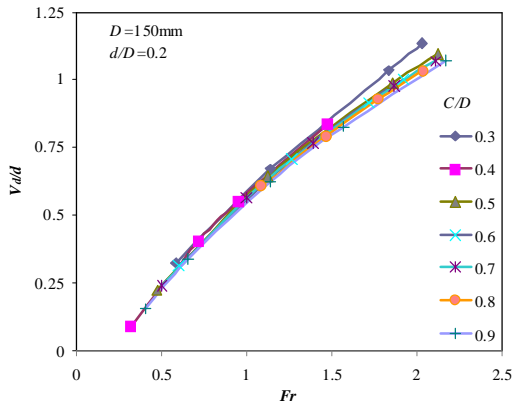
3.1. Effects of Impeller Depth

As mentioned in Eq. (9), the vortex depth is also a function of impeller clearance depth, so relative vortex depth (V_d/d) against Fr at various C/D for a constant impeller diameter is plotted in Fig 2. Vortex depth increases with the increase in Froude number. It is observed that vortex depth also varies at different impeller clearance depth when impeller diameter is constant (Fig. 2). However, it is evidently that the closer is impeller to tank bottom, the higher is vortex depth. Markopoulos and Kontogeorgaki [6] expressed that the significance of C/D on the determination of V_d/d is not essential in a single impeller system and such finding is also witnessed from our study.

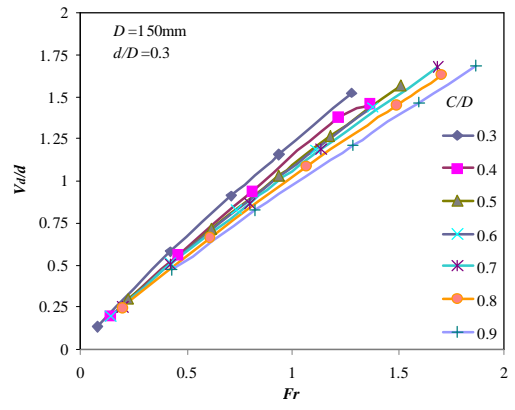
3.2. Effects of Impeller Diameter

(a) *When d is varied:* As vortex depth is a function of Reynolds number and Froude number (Eq. (9)), the diameter of impeller d is very important geometrical parameter to understand the vortex depth. Fig. 3 shows the relative vortex depth vs. Froude number for different impeller diameters at a particular impeller clearance. Vortex depth increases with the increase in the impeller diameter in all the cases of impeller clearance ($C/D=0.3, 0.6$ and 0.9). So, the highest value of V_d/d is observed at $d/D=0.4$ (higher d value when D is constant) and the lowest one at $d/D=0.2$.

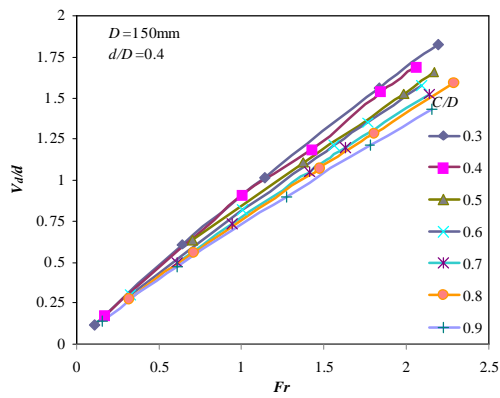
(b) *When d is constant:* As it has been understood from the previous observation, the relative vortex depth increases with the increase in the impeller diameter when the tank diameter is constant. Now it is also interesting to understand how the relative vortex acts when the condition is reversed. So, Fig. 4 shows the comparison of relative vortex depth for two different tank diameters (150 and 200 mm) when the impeller diameter is constant ($d = 60$ mm) at different impeller clearance depth. In all cases of impeller clearance depth ($C/D = 0.3, 0.6$ and 0.9), V_d/d is observed to be higher at the smaller tank diameter, i.e. $D = 150$ mm when d is constant.



a)

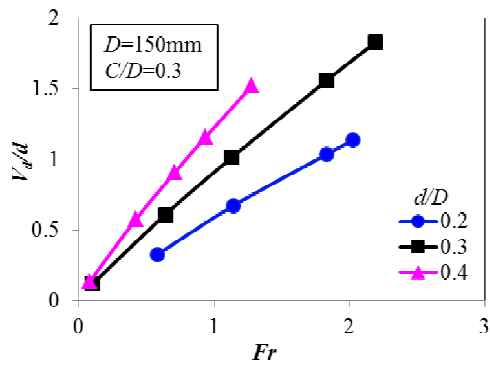


b)

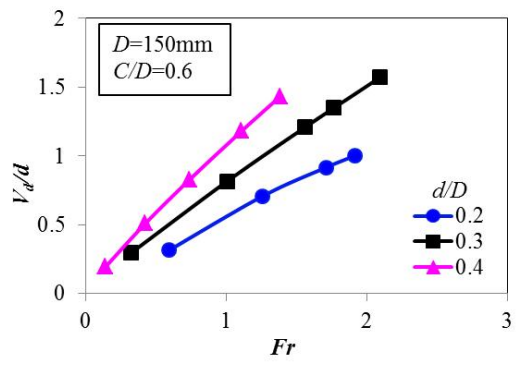


c)

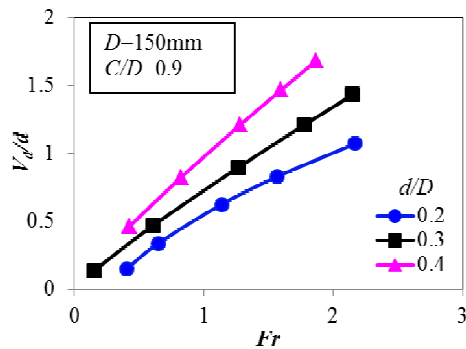
Fig. 2. Relative vortex depth (V_d/d) vs. various Fr for different C/D at $d/D = 0.2$ (a); $d/D = 0.3$ (b) and $d/D = 0.4$ (c)



a)



b)



c)

Fig. 3. Relative vortex depth (V_d/d) vs. Fr

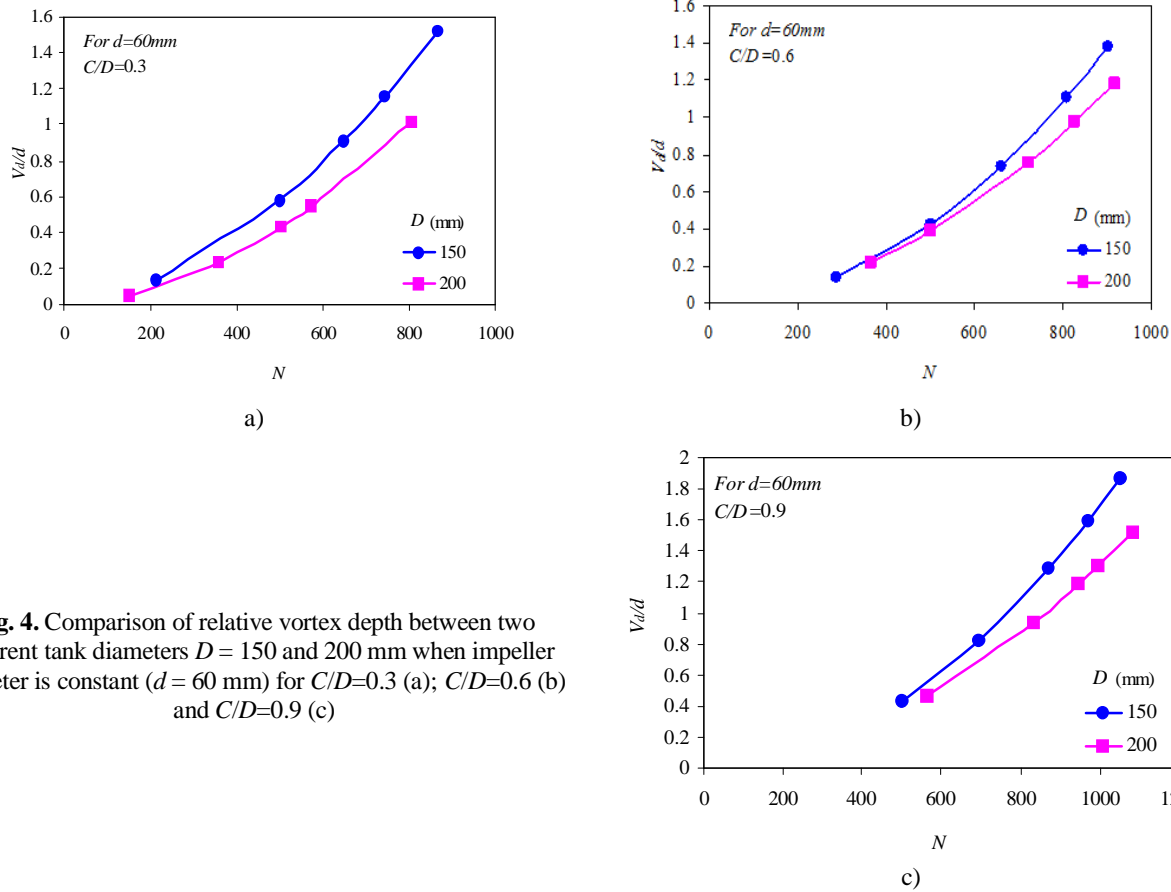


Fig. 4. Comparison of relative vortex depth between two different tank diameters $D = 150$ and 200 mm when impeller diameter is constant ($d = 60$ mm) for $C/D=0.3$ (a); $C/D=0.6$ (b) and $C/D=0.9$ (c)

3.3. Critical Speed

The critical impeller speed N_c is the speed of the stirrer at which the vortex reached the blade level and the air-entrainment occurred. This impeller speed is the most important parameter from the practical point of view because the gas entrainment at this speed is a result of the gas/liquid interface reaching the impeller [29]. The knowledge of the critical impeller speed helps in setting the process at optimal level. Rieger *et al.* [29] have found that better conditions prevail for mass transfer process at above critical speed. However, in order to avoid aeration and vibration, the process setting below critical speed is desired. In the scale up process, when the large scale is used, the swirling and unstable flow conditions are observed when the central vortex reaches the impeller; it can also give rise to mechanical damage [3]. Conversion of impeller rotation kinetic energy to the potential energy (depth of vortex) can be used to determine the critical speed. According to Tsao [30], kinetic energy can be expressed in terms of the speed at the tip of the rotating blades. The energy balance is shown in Eq. (11):

$$V_d r g = k(p^2 d^2 N^2 r) / 2 \quad (11)$$

or it can be written as follows:

$$\frac{V_d}{d} = k \frac{N^2 d}{g} = k F_r \quad (12)$$

The value of k can be derived by analyzing the observations of vortex depth and Froude number of the stirred tanks shown in Fig. 2. Fig. 4 shows the calculated critical impeller speed at different impeller clearance depth for different d/D ratio. This shows that N_c decreases with the increase in C/D and d/D . That means larger the impeller diameter, lower is the critical speed when the tank diameter is constant. Markopoulos and Kontogeorgaki [6] reviewed various experimental results and correlations of relative vortex depth and concluded that the critical impeller speed increases with increasing D/d value. That means N_c increases with either increasing D when d is constant or decreasing d when D is constant. And the same pattern is achieved in this study too as can be seen from Fig. 5. N_c is closely associated with d and D and commonly studied based on ratio of these two variables in order to understand the scale effects. The reason for increasing N_c with the increase in D or decrease in d when another variable is kept constant, may be because of the fact that N_c is the speed when the vortex reaches the upper impeller blade, as mentioned above. It is obvious that higher d produces

Statistical details of Eq. (13)

a	β	γ	δ	η	λ	f	Std. error
0.63 ($1.23 \cdot 10^{-1}$)	0.069 ($2.11 \cdot 10^{-2}$)	-1.395 ($7.32 \cdot 10^{-2}$)	1.14 ($1.02 \cdot 10^{-2}$)	-0.008 ($4.56 \cdot 10^{-3}$)	0.008 ($1.16 \cdot 10^{-3}$)	-0.79 ($1.15 \cdot 10^{-2}$)	$1.3627 \cdot 10^{-2}$

deeper V_d leading to reach the blade level faster than the lower d value while maintaining the same speed. In the case of higher D value when d is constant the case is reversed, which means that the vortex of higher D requires higher speed to reach the blade level compared with the lower D while constants N and d are still maintaining and this leads to the increase in N_c .

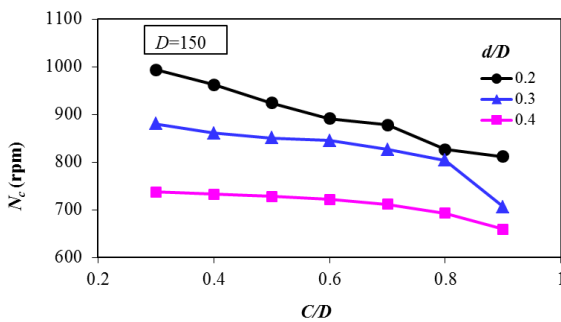


Fig. 5. Critical speed N_c for different d/D at various impeller clearance depth (C/D)

3.4. Scale up Criteria for Vortex Depth

It is shown in Eq. (10) that vortex depth is the function of Reynolds number and Froude number with diameter of impeller and impeller clearance depth. To establish a generalized scale criterion for vortex depth considering the parameters which affects them it can be written as:

$$\frac{V_d}{d} = aGa^b (D/d)^g Fr^{dGa^h (D/d)^g} (C/D)^f \quad (13)$$

The statistical details of the developed relation are tabulated in Table 2. The standard error obtained is found to be satisfactory. The R^2 value is 0.81 and it is the acceptable value in engineering applications of predicted parameters. Fig. 6 shows the overall generalized relationship of predicted V_d/d with observed V_d/d .

With constant $C/D = 1/3$, Reiger *et al.* [29] have developed the vortex depth relationship for different types of impeller (disc blade, flat blade, pitched blade). They found the constants $\alpha = 1.51 \pm 0.03$; $\beta = 0.069$; $\gamma = -0.38$; $\delta = 1.14$; $\eta = -0.008$; $\lambda = 0.008$. Present relationship which is given in Eq. (13) has found similar constant values after the inclusion of C/D , except the value of α and φ and the extra f values. Such modification may be due to different impellers employed in the present work and the inclusion of impeller clearance. So, Eq. (11) is valid for the

following conditions: $D/d = 2.5-5$; $l/d = 0.25$; $b/d = 0.2$; $C/D = 0.3-0.9$ and $H/D = 1$.

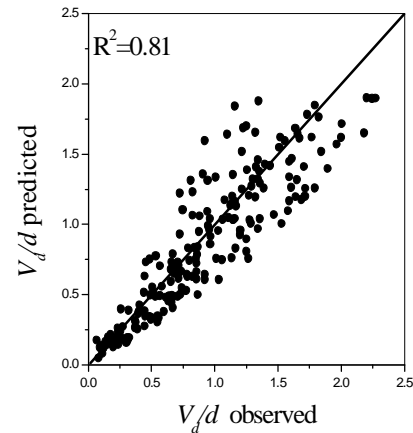


Fig. 6. Parity plot of relative vortex depth correlation for unbaffled stirred tanks

4. Conclusions

The influence of geometrical dimensions and impeller speed on the vortex depth has been studied in an unbaffled single impeller system. Scale up criteria for relative vortex depth has also been developed which is applicable for geometrically similar systems. Relative vortex depth V_d/d increases with the increase in Froude number. There is no significant variation of relative vortex depth with changing the impeller clearance in all the cases of different ratio between impellers diameter to tank diameter ($d/D = 0.2, 0.3$ and 0.4). However, it can be seen that if the impeller is closer to the tank bottom, the vortex depth is higher. Relative vortex depth increases with the increase in impeller diameter in all the cases of impeller clearance ($C/D = 0.3, 0.6$ and 0.9) at constant D . Smaller tank diameter, *i.e.* $D = 150$ mm gives higher relative vortex depth as compared with 20mm when d is constant at different impeller clearance depth. Critical speed N_c is found decreasing with the increase in C/D and d/D . That means larger the impeller diameter, lower is the critical speed when the tank diameter is constant. Scale up criteria for V_d/d has been developed, which is valid for geometric conditions of $H/D = 1$, $n = 6$, $l/d = 0.25$, $b/d = 0.2$ of the turbulent flow when water is used as an operating fluid.

Symbols

a, b, g, d, h, l, f, f – derived constants
 p_0 – atmospheric pressure, N/m²
 r_w – density of water, kg/m³
 x_L – geometric length parameter
 \hat{n} – normal tensor
 s – shear stress, N/m²
 b – width of blade, m
 C – impeller clearance depth, m
 D – diameter of tank, m
 d – impeller diameter, m
 $Fr = Nd^2/g$ – Froude number
 $g = 9.81$ – acceleration of gravity, m/s²
 $Ga = Re^2/Fr$ – Galileo number

H – height of water, m
 l – length of blade, m
 N – impeller speed, s⁻¹
 n – number of rotor blades
 N_C – critical speed, s⁻¹
 p – pressure, N/m²
 $Re = Nd^2/\nu$ – Reynolds number
 t – time, s
 v – velocity, m/s
 V_d – vortex depth, m
 w – thickness of blade, m
 x – geometric parameter
 x_L – coordinate of the liquid surface

References

- [1] Nagata S.: *Mixing: Principles and Applications*. Wiley, New York 1975.
- [2] Glover G., Fitzpatrick J.: *Chem. Eng. J.*, 2013, **127**, 11. <https://doi.org/10.1016/j.cej.2006.09.019>
- [3] Assirelli M., Bujalski W., Eaglesham A., Nienow A.: *Chem. Eng. Sci.*, 2014, **63**, 35. <https://doi.org/10.1016/j.ces.2007.07.074>
- [4] Kumar B.: *Chem. React. Eng. Catalysis*, 2009, **4**, 55.
- [5] Markopoulos J., Kontogeorgaki E.: *Chem. Eng. Techn.*, 1995, **18**, 68. <https://doi.org/10.1002/ceat.270180113>
- [6] Pacek A., Ding P., Nienow A.: *Chem. Eng. Sci.*, 2001, **56**, 3247. [https://doi.org/10.1016/S0009-2509\(01\)00015-X](https://doi.org/10.1016/S0009-2509(01)00015-X)
- [7] Hekmat D., Hebel D., Schmid H., Weuster-Botz D.: *Process Biochem.*, 2007, **42**, 1649. <https://doi.org/10.1016/j.procbio.2007.10.001>
- [8] Aloï L., Cherry R.: *Chem. Eng. Sci.*, 1996, **51**, 1523. [https://doi.org/10.1016/0009-2509\(95\)00307-X](https://doi.org/10.1016/0009-2509(95)00307-X)
- [9] Rousseau J., Muhr H., Plasari E.: *Can. J. Chem. Eng.*, 2001, **79**, 697. <https://doi.org/10.1002/cjce.5450790501>
- [10] Pinelli D., Nocentini M., Magelli F.: *Chem. Eng. Commun.*, 2001, **188**, 91. <https://doi.org/10.1080/00986440108912898>
- [11] Abatan A., McCarthy J., Vargas W.: *AIChE J.*, 2006, **52**, 2039. <https://doi.org/10.1002/aic.10834>
- [12] Montante G., Paglianti A., Magelli F.: 12th Eur. Conf. on Mixing, Bologna, AIDIC, Milan 2006 137.
- [13] Rao A., Kumar B.: *J. Chem. Technol. Biotechnol.*, 2007, **82**, 101. <https://doi.org/10.1002/jctb.1643>
- [14] Tezura S., Kimura A., Yoshida M *et al.*: *J. Chem. Technol. Biotechnol.*, 2007, **82**, 672. <https://doi.org/10.1002/jctb.1726>
- [15] Galletti C., Brunazzi E.: *Chem. Eng. Sci.*, 2008, **63**, 4494. <https://doi.org/10.1016/j.ces.2008.06.007>
- [16] Shan X., Yu G., Yang C., Mao Z.: *Chinese J. Process. Eng.*, 2008, **8**, 1.
- [17] Yoshida M., Kimura A., Yamagiwa K. *et al.*: *J. Fluid. Sci. Technol.*, 2008, **3**, 282. <https://doi.org/10.1299/jfst.3.282>
- [18] Hirata Y., Dote T., Inoue Y.: *Chem. Eng. Res. Des.*, 2009, **87**, 430. <https://doi.org/10.1016/j.cherd.2008.12.022>
- [19] Brucato A., Cipollina A., Micale G. *et al.*: *Chem. Eng. Sci.*, 2010, **65**, 3001. <https://doi.org/10.1016/j.ces.2010.01.026>
- [20] Tamburini A., Cipollina A., Micale G. *et al.*: *Chem. Eng. J.*, 2012, **193-194**, 234. <https://doi.org/10.1016/j.cej.2012.04.044>
- [21] Tamburini A., Cipollina A., Micale G., Brucato A.: *Chem. Eng. Transact.*, 2011, **24**, 1441. <https://doi.org/10.3303/CET1124241>
- [22] Wang B., Lan C., Horsman M.: *Biotech. Adv.*, 2012, **30**, 904. <https://doi.org/10.1016/j.biotechadv.2012.01.019>
- [23] Grisafi F., Brucato A., Rizzuti L.: *ICChemE Symp. Ser.*, 1994, **136**, 571.
- [24] Rao A., Kumar B.: *J. Hydraul. Eng. ASCE*, 2009, **135**, 38. [https://doi.org/10.1061/\(ASCE\)0733-9429\(2009\)135:1\(38\)](https://doi.org/10.1061/(ASCE)0733-9429(2009)135:1(38))
- [25] Rieger F., Ditl P., Noval V.: *Chem. Eng. Sci.*, 1979, **34**, 397. [https://doi.org/10.1016/0009-2509\(79\)85073-3](https://doi.org/10.1016/0009-2509(79)85073-3)
- [26] Tsao G.: *Biotechnol. Bioeng.*, 1968, **10**, 177. <https://doi.org/10.1002/bit.260100206>

Received: May 30, 2016 / Revised: June 29, 2016 / Accepted: December 02, 2016

АНАЛІЗ ГЛИБИНИ ВИХОРУ В НЕЕКРАНОВАНОМУ РЕЗЕРВУАРІ З ПЕРЕМІШУВАННЯМ І ЛОПАТЕВИМ ІМПЕЛЕРОМ

Анотація. Проведені дослідження в неекранованому резервуарі з перемішуванням, обладнаним імπεлером з увігнутими лопатями. Вивчено вплив діаметра робочого колеса (d), діаметру резервуара (D) і глибини зазору робочого колеса (C) на глибину вихорів за різних швидкостей обертання імπεлера. Визначено, що глибина вихору є більшою, коли робоче колесо знаходиться ближче до дна резервуара. Відносна глибина вихору збільшується зі збільшенням діаметра робочого колеса при всіх значеннях глибини зазору робочого колеса при постійному D . Встановлено, що при постійному d і різній глибині зазору робочого колеса чим менший діаметр резервуара, тим більша відносна глибина вихору. Критична швидкість змінюється зі збільшенням C/D і d/D . Розроблено масштабований критерій відносної глибини вихору, дійсний для геометрично подібних умов.

Ключові слова: увігнута лопать, обчислювальна гідродинаміка, резервуар з мішалкою, глибина вихору.